Journal of Ethnopharmacology 162 (2015) 231–237

Contents lists available at ScienceDirect

Journal of Ethnopharmacology

journal homepage: www.elsevier.com/locate/jep

Research Paper

Identification of cytotoxic and anti-inflammatory constituents from the bark of *Toxicodendron vernicifluum* (Stokes) F.A. Barkley

Ki Hyun Kim [a], Eunjung Moon [b], Sang Un Choi [c], Changhyun Pang [d], Sun Yeou Kim [b], Kang Ro Lee [a,*]

[a] Natural Products Laboratory, School of Pharmacy, Sungkyunkwan University, Suwon 440-746, Republic of Korea
[b] College of Pharmacy, Gachon University, #191 Hambakmoero, Yeonsu-gu, Incheon 406-799, Republic of Korea
[c] Korea Research Institute of Chemical Technology, Deajeon 305-600, Republic of Korea
[d] School of Chemical Engineering, Sungkyunkwan University, Suwon 440-746, Republic of Korea

ARTICLE INFO

Article history:
Received 16 September 2014
Received in revised form
26 December 2014
Accepted 30 December 2014
Available online 9 January 2015

Keywords:
Toxicodendron vernicifluum
Anacardiaceae
Polyphenols
Flavonoids
Anti-tumor activity
Anti-inflammation

Chemical compounds studied in this article:
(+)-(2*S*,3*R*)-Fustin (PubChem CID: 72282)
(+)-Epitaxifolin (PubChem CID: 443758)
Sulfuretin (PubChem CID: 5281295)
Butein (PubChem CID: 5281222)
Fisetin (PubChem CID: 5281614)
Doxorubicin (PubChem CID: 31703)
N^G-monomethyl-L-arginine (PubChem CID: 135242)

ABSTRACT

Ethnopharmacological relevance: *Toxicodendron vernicifluum* (Stokes) F.A. Barkley (Anacardiaceae) has traditionally been used as a food supplement and in traditional herbal medicine to treat inflammatory diseases and cancers for centuries in Korea. This study was designed to isolate the bioactive constituents from the ethanol extract of *Toxicodendron vernicifluum* bark and evaluate their cytotoxic and anti-inflammatory activities.

Material and methods: Bioassay-guided fractionation and chemical investigation of the ethanol extract of *Toxicodendron vernicifluum* bark resulted in the isolation and identification of three new polyphenols (**1–3**) and six flavonoids (**4–9**). The structures of the isolated compounds were elucidated by spectroscopic analysis, including 1D and 2D nuclear magnetic resonance (NMR) (^{1}H, ^{13}C, COSY, HMQC and HMBC experiments), and high resolution (HR)-mass spectrometry, and their absolute configurations were further confirmed by chemical methods and circular dichroism (CD) data analysis. Compounds **1–9** were evaluated for their antiproliferative activities against four human tumor cell lines (A549, SK-OV-3, SK-MEL-2, and HCT-15), and anti-inflammatory activities by measuring nitric oxide (NO) levels in the medium of murine microglia BV-2 cells.

Results: The isolated compounds were characterized as in the following: three new polyphenols, rhusopolyphenols G-I (**1–3**) and six flavonoids including two aurones, 2-benzyl-2,3′,4′,6-tetrahydroxybenzo[*b*]furan-3(2*H*)-one (**4**), sulfuretin (**5**), two dihydroflavonols, (+)-(2*S*,3*R*)-fustin (**6**), (+)-epitaxifolin (**7**), one chalcone, butein (**8**), and one flavonol, fisetin (**9**). The published NMR assignments of **4** were corrected by the detailed analysis of spectroscopic data in this study. Among the tested compounds, compounds **4–9** showed antiproliferative activity against the tested cells, with IC_{50} values of 4.78–28.89 μM. Compounds **5** and **8** significantly inhibited NO production in lipopolysaccharide (LPS)-stimulated BV-2 cells with IC_{50} values of 23.37 and 11.68 μM, respectively.

Conclusions: Polyphenols including flavonoids were one of the main constituents of *Toxicodendron vernicifluum* bark, and activities demonstrated by the isolated compounds support the ethnopharmacological use of *Toxicodendron vernicifluum* as anti-cancer and/or anti-inflammatory agents.

1. Introduction

Toxicodendron vernicifluum (Stokes) F.A. Barkley (formerly *Rhus verniciflua* Stokes, Anacardiaceae), the lacquer tree, is an indigenous East Asian plant. *Toxicodendron vernicifluum* bark has traditionally been used as a food supplement and in traditional herbal medicine for treating abdominal disorders such as dyspepsia, abdominal pain, abdominal infection, and heartburn, and inflammatory diseases including arthritis, bronchitis, and neuralgia (Huh, 1999; Kim, 2000; Lee et al., 2010). It has also been used to treat cancers, particularly stomach and uterine cancers in South Korea since the 15th century (Huh, 1999). The medicinal use of this tree

Abbreviations: NMR, nuclear magnetic resonance; CD, circular dichroism; SRB, sulforhodamine B; NO, nitric oxide; LPS, lipopolysaccharide; IR, infrared; UV, ultraviolet; HR, high resolution; ESI, electrospray ionization; MS, mass spectrometry; COSY, correlation spectroscopy; HMQC, heteronuclear multiple quantum coherence; HMBC, heteronuclear multiple bond correlation; HPLC, preparative high performance liquid chromatography; RP, reversed-phase; TLC, thin-layer chromatography; CC, column chromatography; DMEM, Dulbecco's modified Eagle medium; FBS, fetal bovine serum; NCI, national cancer institute; MTT, 3-[4, 5-dimethylthiazol-2-yl]-2, 5-diphenyl-tetrazolium bromide; L-NMMA, N^G-monomethyl-L-arginine; NOS, nitric oxide synthase

* Correspondence to: Natural Products Laboratory, School of Pharmacy, Sungkyunkwan University, 300 Chonchon-dong, Jangan-ku, Suwon 440-746, Korea. Tel.: +82 31 290 7710; fax: +82 31 290 7730.
E-mail address: krlee@skku.edu (K.R. Lee).

http://dx.doi.org/10.1016/j.jep.2014.12.071
0378-8741/

has been limited because it contains the allergen, urushiol, which causes severe dermatitis. After boiling the bark with other foods such as chicken and duck to alleviate its toxicity, whole dish cooked with herb and poultry is eaten to acquire its beneficial effects (Lee et al., 2010).

In recent preclinical studies of this tree by a number of investigators, the extract of *Toxicodendron vernicifluum* exhibited antiproliferative and apoptotic activities in various human cancer cell lines via activation of caspase-9 and inhibition of the PI3KAkt/PKB pathway, as well as antioxidant effects (Lee et al., 2002, 2009; Jang et al., 2005; Son et al., 2005; Samoszuk et al., 2005; Kim et al., 2008, 2009). In our continuing search for bioactive constituents from Korean medicinal plants, we also confirmed the potential of *Toxicodendron vernicifluum* bark as an anticancer agent based on the fact that the EtOH extract of *Toxicodendron vernicifluum* had excellent cytotoxic activity against A549, SK-OV-3, SK-MEL-2, and HCT-15 cell lines with IC_{50} values of 15.82, 10.10, 7.58, and 8.35 μM, respectively using a sulforhodamine B (SRB) bioassay in our screening test. Furthermore, our preliminary study confirmed that the EtOH extract had a significant inhibitory effect on nitric oxide (NO) production in a dose-dependent manner in the lipopolysaccharide (LPS)-stimulated BV-2 microglial cell line, which is associated with anti-inflammatory effect of *Toxicodendron vernicifluum*. But few reports have emphasized the active constituents responsible for the cytotoxic and anti-inflammatory effects of this tree.

Therefore, in the course of our study to prove the ethnopharmacological use of *Toxicodendron vernicifluum* as anti-cancer and/or anti-inflammatory agents, we reported 10 polyphenols that correlated with the cytotoxic and anti-inflammatory activities from the *Toxicodendron vernicifluum* bark in our recent study (Kim et al., 2013). In the process of our continuing efforts to study this source, we further isolated three new polyphenols (**1–3**) and six known flavonoids (**4–9**) (Fig. 1) from the active fractions using a bioassay-guided fractionation method. This paper reports the isolation and structural elucidation of compounds **1–9** and their cytotoxic and anti-inflammatory activities.

2. Material and methods

2.1. General

Optical rotations were measured on a Jasco P-1020 polarimeter using methanol or acetone as a solvent. Infrared (IR) spectra were recorded on a Bruker IFS-66/S FT-IR spectrometer. Circular dichroism (CD) spectra were measured on a JASCO J-810 spectropolarimeter. Ultraviolet (UV) spectra were recorded with a Shimadzu UV-1601 UV–visible spectrophotometer. high resolution (HR)-electrospray ionization mass spectrometry (ESIMS) and ESIMS spectra were recorded on a Micromass QTOF2-MS. Nuclear magnetic resonance (NMR) spectra, including the spectra in the ^1H–^1H correlation spectroscopy (COSY), heteronuclear multiple quantum coherence (HMQC), and heteronuclear multiple bond correlation (HMBC) experiments, were recorded on a Varian UNITY INOVA 500 NMR spectrometer operating at 500 MHz (^1H) and 125 MHz (^{13}C), with chemical shifts given in ppm (δ). Preparative high performance liquid chromatography (HPLC) used a Gilson 306 pump with a Shodex refractive index detector. Silica gel 60 (Merck, 230–400 mesh) and reversed-phase (RP)-C_{18} silica gel (Merck, 230–400 mesh) were used for column chromatography. The packing material for molecular sieve column chromatography was Sephadex LH-20 (Pharmacia Co. Ltd.). Merck precoated silica gel F_{254} plates and RP-18 F_{254s} plates were used for thin-layer chromatography (TLC). Spots were detected on TLC under UV light or by heating after spraying with anisaldehyde–sulfuric acid.

2.2. Plant material

Toxicodendron vernicifluum bark was collected in Hoengseong, Gangwon-do, Korea, in March 2010. The plant material was identified by one of the authors (K. R. Lee). A voucher specimen (SKKU-RV 2010_3) was deposited at the Farm Corporation, Dongyi's Farms, Boryung, Chungcheongnam-do, Korea.

2.3. Extraction and isolation

The air-dried and pulverized plant material (1.3 kg) was soaked in distilled H_2O refluxed for 1 h, and then cooled. The material in H_2O was fermented in *Aspergillus ortzae* at 30 °C for 35 h to augment the active constituents and remove the allergen, urushiol (Kim et al., 2011). The fermented material was extracted with H_2O twice (each 20 L × 3 h) under reflux and filtered. The filtrate was evaporated under vacuum to obtain a crude extract (120 g), which was further extracted with EtOH to yield a crude EtOH extract (60 g). The EtOH extract (10 g) was subjected to C_{18} reverse-phased silica gel column chromatography (CC), eluted with a gradient of MeOH–H_2O (2:3→1:0) to yield six fractions (A–F). Each fraction was evaluated for cytotoxic activity against A549, SK-OV-3, SK-MEL-2, and HCT-15 human tumor cell lines using the SRB bioassay. Fractions B and C showed weak cytotoxicity, whereas fractions D and E exhibited significant cytotoxicity against the tested cell lines. The active fraction B (3.5 g) was chromatographed on Sephadex LH-20 and eluted with

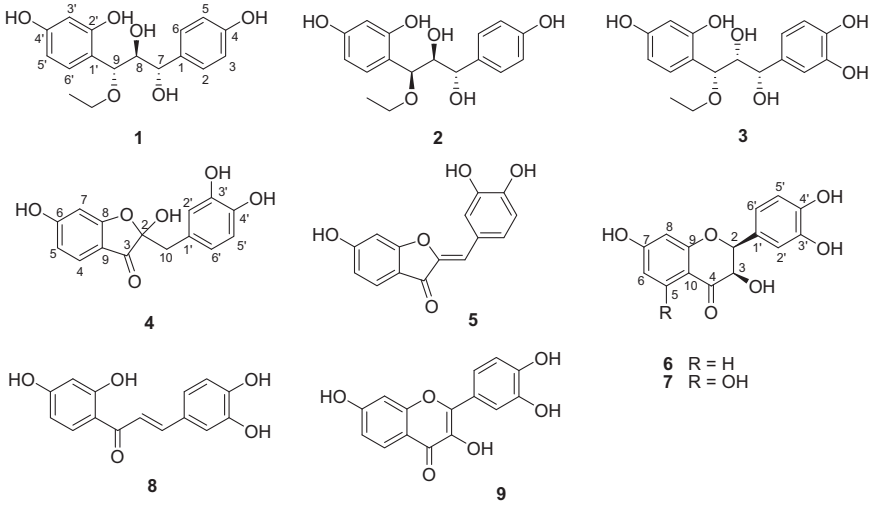

Fig. 1. Chemical structures of compounds **1–9**.

MeOH–H_2O (4:1) to give five subfractions (B1–B5). Fraction B1 (130 mg) was further purified by semi-preparative HPLC using a solvent system of MeCN–H_2O (1:4) at a flow rate of 2.0 mL/min (Econosil RP-18 column; 250 × 10 mm^2; 10 μm particle size; Shodex refractive index detector) to give **4** (t_R=15.4 min, 15 mg). Compound **6** (t_R=13.5 min, 7 mg) was isolated from fraction B2 (85 mg) by the purification of semi-preparative HPLC, as described above, using a solvent system of MeOH–H_2O (2:3). Next, the active fraction C (550 mg) was subjected to Sephadex LH-20 chromatography, eluted with MeOH–H_2O (4:1) to afford five subfractions (C1–C5). Fraction C4 (130 mg) was purified by semi-preparative HPLC using a solvent system of MeOH–H_2O (9:11) to yield **7** (t_R=15.1 min, 4 mg). The active fraction D (560 mg) was chromatographed on a silica gel CC and eluted with $CHCl_3$–MeOH (17:1) to give six subfractions (D1–D6). Fraction D2 (155 mg) was purified by semi-preparative HPLC, using a solvent system of MeCN–H_2O (3:7) to yield **1** (t_R=15.8 min, 12 mg) and **2** (t_R=16.2 min, 5 mg). Fraction D5 (45 mg) was also purified using semi-preparative HPLC with a solvent system of MeOH–H_2O (47:53) to yield **3** (t_R=14.2 min, 5 mg). Finally, active fraction E (1.9 g) was separated over a silica gel CC and eluted with $CHCl_3$–MeOH (15:1) to yield five subfractions (E1–E5). Fraction E3 (350 mg) was purified by semi-preparative HPLC, using a solvent system of MeOH–H_2O (3:2) to give **5** (t_R=16.3 min, 10 mg) and **8** (t_R=14.2 min, 6 mg). Fraction E5 (800 mg) was further separated by C_{18} reverse-phased silica gel CC and eluted with increasing MeOH in H_2O to yield two subfractions (E51 and E52). Fraction E52 (110 mg) was purified by semi-preparative HPLC, using a solvent system of MeOH–H_2O (3:2) to obtain **9** (t_R=14.1 min, 15 mg).

2.3.1. Rhusopolyphenol G (**1**)

Colorless gum; $[\alpha]_D^{25}$ +25.5 (*c* 0.35, MeOH); UV (MeOH) λ_{max} nm (log ε): 218 (3.9), 275 (2.5); CD (MeOH): $[\theta]_{246}$ −13,300, $[\theta]_{294}$ +1800; IR (KBr) ν_{max} cm^{-1}: 3405, 2945, 2835, 2504, 1645, 1450, 1120, and 1030; ^1H (500 MHz) and ^{13}C (125 MHz) NMR data, see Table 1; ESIMS (positive-ion mode) *m/z* 343 $[M+Na]^+$; HR-ESIMS (positive-ion mode) *m/z* 343.1163 $[M+Na]^+$ (calcd. for $C_{17}H_{20}O_6Na$, 343.1158).

2.3.2. Rhusopolyphenol H (**2**)

Colorless gum; $[\alpha]_D^{25}$ −15.7 (*c* 0.15, MeOH); UV (MeOH) λ_{max} nm (log ε): 218 (3.9), 275 (2.6); CD (MeOH): $[\theta]_{235}$ −21,400, $[\theta]_{280}$ −28,300; IR (KBr) ν_{max} cm^{-1}: 3402, 2945, 2836, 2504, 1653, 1450, 1120, and 1031; ^1H (500 MHz) and ^{13}C (125 MHz) NMR data, see Table 1; ESIMS (positive-ion mode) *m/z* 343 $[M+Na]^+$; HR-ESIMS (positive-ion mode) *m/z* 343.1159 $[M+Na]^+$ (calcd. for $C_{17}H_{20}O_6Na$, 343.1158).

2.3.3. Rhusopolyphenol I (**3**)

Colorless gum; $[\alpha]_D^{25}$ −13.8 (*c* 0.15, MeOH); UV (MeOH) λ_{max} nm (log ε): 218 (4.1), 274 (2.6); IR (KBr) ν_{max} cm^{-1}: 3405, 2945, 2835, 2510, 1655, 1450, 1120, and 1031; ^1H (500 MHz) and ^{13}C (125 MHz) NMR data, see Table 1; ESIMS (positive-ion mode) *m/z* 359 $[M+Na]^+$; HR-ESIMS (positive-ion mode) *m/z* 359.1103 $[M+Na]^+$ (calcd for $C_{17}H_{20}O_7Na$, 359.1107).

2.3.4. 2-Benzyl-2,3′,4′,6-tetrahydroxybenzo[b]furan-3(2H)-one (**4**)

Yellowish powder; $[\alpha]_D^{25}$ 0 (*c* 0.50, MeOH); ^1H (500 MHz) and ^{13}C (125 MHz) NMR data, see Table 2; ESIMS (positive-ion mode) *m/z* 311 $[M+Na]^+$.

Table 2
^1H (500 MHz) and ^{13}C NMR (125 MHz) data of compounds **4** and **6** in CD_3OD (δ in ppm, *J* values in parentheses)[a].

No.	**4**		**6**	
	δ_H (*J* in Hz)	δ_C	δ_H (*J* in Hz)	δ_C
2		106.1	5.35 d (3.0)	81.8
3		197.8	4.30 d (3.0)	72.4
4	7.30 d (8.5)	125.6		191.4
5	6.40 dd (8.5, 2.0)	111.2	7.72 d (8.5)	128.8
6		168.2	6.53 dd (8.5, 2.5)	110.5
7	6.27 d (2.0)	97.4		165.4
8		173.3	6.40 d (2.5)	102.4
9		118.8		163.4
10	3.08 d (14.0); 3.04 d (14.0)	40.9		112.1
1′		124.8		127.5
2′	6.63 d (2.0)	117.3	6.99 d (2.0)	114.5
3′		144.2		144.6
4′		143.7		145.0
5′	6.53 d (8.5)	114.4	6.75 d (8.5)	114.6
6′	6.48 dd (8.5, 2.0)	121.6	6.82 dd (8.5, 2.0)	118.7

[a] The assignments were based on ^1H,^1H-COSY, HMQC and HMBC experiments.

Table 1
^1H (500 MHz) and ^{13}C NMR (125 MHz) data of rhusopolyphenols G-I (**1–3**) in CD_3OD (δ in ppm, *J* values in parentheses)[a].

No.	**1**		**2**		**3**	
	δ_H (*J* in Hz)	δ_C	δ_H (*J* in Hz)	δ_C	δ_H (*J* in Hz)	δ_C
1		129.2		130.0		130.4
2	7.27 dd (8.5, 2.0)	129.0	7.28 dd (8.5, 2.0)	128.7	6.99 d (2.0)	114.3
3	6.80 dd (8.5, 2.0)	114.8	6.81 dd (8.5, 2.0)	114.6		144.7
4		157.5		157.1		144.9
5	6.80 dd (8.5, 2.0)	114.8	6.81 dd (8.5, 2.0)	114.6	6.78 d (8.5)	114.8
6	7.27 dd (8.5, 2.0)	129.0	7.28 dd (8.5, 2.0)	128.7	6.81 dd (8.5, 2.0)	118.2
7	4.66 d (10.0)	81.6	5.04 d (9.5)	76.9	4.97 d (1.0)	75.2
8	3.92 dd (10.0, 7.0)	72.2	3.99 dd (9.5, 3.0)	70.2	3.95 dd (2.5, 1.0)	68.7
9	4.55 d (7.0)	79.6	4.32 d (3.0)	74.3	4.17 d (2.5)	75.6
1′		114.4		112.4		111.2
2′		155.8		155.2		156.2
3′	6.22 d (2.0)	102.1	6.28 d (2.0)	102.1	6.36 d (2.0)	102.6
4′		158.1		158.9		158.6
5′	6.42 dd (8.5, 2.0)	108.9	6.40 dd (8.5, 2.0)	107.5	6.42 dd (8.5, 2.0)	108.4
6′	7.18 d (8.5)	128.9	7.08 d (8.5)	131.1	7.11 d (8.5)	132.7
OEt	3.88 q (7.5)	65.5	3.74 q (7.5)	64.2	3.75 q (7.5)	63.9
	3.77 q (7.5)		3.70 q (7.5)		3.71 q (7.5)	
	1.24 t (7.5)	14.7	1.25 t (7.5)	14.2	1.24 t (7.5)	14.7

[a] The assignments were based on ^1H,^1H-COSY, HMQC and HMBC experiments.

*2.3.5. (+)-(2S,3R)-Fustin (**6**)*

Amorphous solid; $[\alpha]_D^{25}$ +35.1 (*c* 0.30, MeOH); ^{1}H (500 MHz) and ^{13}C (125 MHz) NMR data, see Table 2; ESIMS (positive-ion mode) *m/z* 311 $[M+Na]^+$.

2.4. Mitsunobu reaction

Ph_3P (2 mg, 0.008 mmol) was added to a solution of compound **3** (1.6 mg, 0.005 mmol) in anhydrous THF (0.05 ml). The mixture was stirred for 15 min, and DEAD (Diethyl azodicarboxylate) (1.5 μl, 0.008 mmol) was added dropwise to the reaction mixture. After stirring for 3 h at room temperature (reaction monitored by TLC), the reaction mixture was diluted with EtOAc (5 ml) and washed with H_2O (5 ml) and brine (4 ml). The organic phase was dried over $MgSO_4$ and filtered and concentrated under reduced pressure to produce a brown residue. The residue was purified with a silica gel Waters Sep-Pak Vac 6 cc (n-Hexane–EtOAc, 3:1) (Water, Milford, MA, USA) to give the cyclized products **3a** as amorphous solids.

*2.4.1. (+)-4-O-Ethyl-mollisacacidin (**3a**)*

Amorphous solid; $[\alpha]_D^{25}$ +38.3 (*c* 0.05, MeOH); CD (MeOH): $[\theta]_{238}$ −53,500, $[\theta]_{290}$ −45,100; IR (KBr) ν_{max} cm^{-1}: 3410, 2940, 1615, 1512, 1241, and 1030; ^{1}H NMR (500 MHz, CD_3OD): δ 7.03 (1H, d, *J*=2.0 Hz, H-2′), 6.89 (1H, d, *J*=8.0 Hz, H-5), 6.86 (1H, dd, *J*=8.5, 2.0 Hz, H-6′), 6.80 (1H, d, *J*=8.5 Hz, H-5′), 6.41 (1H, dd, *J*=8.0, 2.0 Hz, H-6), 6.25 (1H, d, *J*=2.0 Hz, H-8), 5.08 (1H, d, *J*=9.0 Hz, H-2), 4.07 (1H, d, *J*=7.0 Hz, H-4), 3.98 (1H, dd, *J*=9.0, 7.0 Hz, H-3), 3.75 (1H, q, *J*=7.5 Hz, $C\underline{H}_2CH_3$), 3.71 (1H, q, *J*=7.5 Hz, $\underline{CH}_2CH_3$), 1.24 (1H, t, *J*=7.5 Hz, $CH_2C\underline{H}_3$); HR-ESIMS (positive-ion mode) *m/z* 341.1008 $[M+Na]^+$ (calcd. for $C_{17}H_{18}O_6Na$, 341.1001).

2.5. Cell cultures

All tumor cell cultures were maintained using RPMI1640 cell growth medium (Gibco, Carlsbad, CA), supplemented with 5% fetal bovine serum (FBS) (Gibco), 100 units/ml penicillin and 100 μg/ml streptomycin. Human tumor cell lines such as A549 (non-small cell lung carcinoma), SK-OV-3 (ovary malignant ascites), SK-MEL-2 (skin melanoma), and HCT-15 (colon adenocarcinoma) were provided by the National Cancer Institute (NCI). BV2 cells (microglia from murine) were generously provided by Dr. E. Choi from Korea University (Seoul, Korea). It was maintained in Dulbecco's modified Eagle (DMEM) medium supplemented with 5% FBS, 100 units/ml penicillin and 100 μg/ml streptomycin. All cells were incubated at 37 °C in a humidified incubator with 5% CO_2.

2.6. Cytotoxicity assessment

The cytotoxicity of the compounds against cultured human tumor cell lines was evaluated by the SRB method (Skehan et al., 1990). Each tumor cell line was inoculated over standard 96-well flat-bottom microplates and then incubated for 24 h at 37 °C in a humidified atmosphere of 5% CO_2. The attached cells were then incubated with the serially diluted lignan samples. After continuous exposure to the compounds for 48 h, the culture medium was removed from each well and the cells were fixed with 10% cold trichloroacetic acid at 4 °C for 1 h. After washing with tap water, the cells were stained with 0.4% SRB dye and incubated for 30 min at room temperature. The cells were washed again and then solubilized with 10 mM unbuffered Tris base solution (pH 10.5). The absorbance was measured spectrophotometrically at 520 nm with a microtiter plate reader. Doxorubicin (Sigma Chemical Co., ≥98%) was used as the positive control. Doxorubicin had IC_{50} values against A549, SK-OV-3, SK-MEL-2, and HCT15 of 0.016, 0.027, 0.036, and 1.073 μM, respectively.

2.7. Measurement of nitric oxide production and cell viability

BV-2 cells were plated into a 96-well plate (3×10^4 cells/well.). After 24 h, cells were pretreated with compounds **1–9** for 30 min, and then stimulated with 100 ng/ml of LPS for another 24 h. Nitrite, a soluble oxidation product of NO, was measured in the culture media using the Griess reaction. The supernatant was harvested and mixed with an equal volume of Griess reagent (1% sulfanilamide, 0.1% *N*-1-napthylethylenediamine dihydrochloride in 5% phosphoric acid). After 10 min, the absorbance at 570 nm was measured using a microplate reader. Sodium nitrite was used as a standard to calculate the NO_2^- concentration. Cell viability was assessed by a 3-[4, 5-dimethylthiazol-2-yl]-2, 5-diphenyl-tetrazolium bromide (MTT) assay. N^G-monomethyl-L-arginine (L-NMMA, Sigma, St. Louis, MO, USA), a well-known nitric oxide synthase (NOS) inhibitor, was tested as a positive control (Reif and McCreedy, 1995).

3. Results and discussion

3.1. Structure elucidation

Compound **1** was obtained as a colorless gum with positive optical rotation. The molecular formula was established as $C_{17}H_{20}O_6$, based on the positive ion peak at *m/z* 343.1163 $[M+Na]^+$ in the HR-ESIMS (calcd for $C_{17}H_{20}O_6Na$, 343.1158), suggesting eight degrees of unsaturation. The IR absorption spectrum suggested the presence of phenyl (2945 and 1450 cm^{-1}) and hydroxyl (3405 cm^{-1}) groups. The ^{1}H and ^{13}C NMR spectra (Table 1) of **1** were very similar to those of rhusopolyphenol B (Kim et al., 2013), except for the signals attributable to an ethoxy group at δ 3.88 (1H, q, *J*=7.5 Hz), 3.77 (1H, q, *J*=7.5 Hz) and δ 65.5; δ 1.24 (3H, t, *J*=7.5 Hz) and δ 14.7, instead of the methoxyl group present in rhusopolyphenol B. In fact, the double doublet (*J*=10.0 and 7.0 Hz) at δ 3.92, assigned to H-8, showed correlations with two doublets (*J*=10.0 Hz at δ 4.66 and *J*=7.0 Hz at δ_H 4.55) in the ^{1}H–^{1}H correlation spectroscopy (COSY) system, which were assigned to H-7 and H-9 of the 1,2,3-propanetriol chain (Fig. 2). The correlations observed in the heteronuclear multiple-quantum correlation (HMQC) spectrum supported assignment of the signals at δ_C 81.6 (C-7), 72.2 (C-8), and 79.6 (C-9) of the propanetriol chain. The heteronuclear multiple bond correlation (HMBC) correlation between ethoxy protons (δ 3.88 and 3.77) and C-9 (δ 79.6) indicated the presence of the ethoxy group at C-9 (Fig. 2). The gross structure of **1** was established by analysis of the ^{1}H–^{1}H COSY, HMQC, and HMBC spectra (Fig. 2). In the related acyclic polyol derivatives, the trend for larger couplings in *anti*-orientated protons (*J*=7–10 Hz) compared to their *syn*-isomers (*J*=2–3 Hz) has been well established (Wiesler and Nakanishi, 1990), which allowed us to assign the relative configuration of **1** as 7,8-*erythro* and 8,9-*erythro* forms. The absolute configuration of **1** was elucidated to be 7*S*,8*S*,9*R* by comparing its coupling constants, positive specific rotation, and CD data ($[\theta]_{246}$ −13,300, $[\theta]_{294}$ +1800) with those of rhusopolyphenol C ($[\theta]_{250}$ −11,200, $[\theta]_{291}$ +2500) (Kim et al., 2013). Thus, the structure of compound **1** was determined as shown in Fig. 1, and named rhusopolyphenol G.

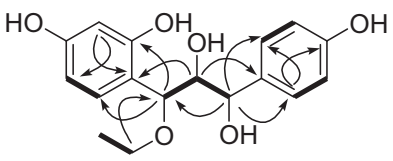

Fig. 2. Key ^{1}H–^{1}H COSY (—) and HMBC (→) correlations of **1**.

Compound **2** was isolated as a colorless gum with negative optical rotation. The HR-ESIMS data showed an ion peak at *m/z* 343.1159 $[M+Na]^+$ (calcd for $C_{17}H_{20}O_6Na$, 343.1158) for the molecular formula $C_{17}H_{20}O_6$ with 8 degrees of unsaturation. The ^1H and ^{13}C NMR spectra (Table 1) were similar to those of **1** with the only differences being the chemical shifts and splitting patterns of C-7 [δ 5.04 (d, J=9.5 Hz); δ 76.9], C-8 [δ 3.99 (dd, J=9.5, 3.0 Hz); δ 70.2], and C-9 [δ 4.32 (d, J=3.0 Hz); δ 74.3] in **2** compared to those of corresponding carbons in **1**. This suggested that compound **2** has different configurations at the 1,2,3-propanetriol moiety from those of compound **1**. The gross structure of **2** was clearly elucidated by analyzing the 2D NMR spectrum (COSY, HMQC, and HMBC). Furthermore, the absolute configuration of **2** was determined to be 7*S*,8*S*,9*S* by comparing its coupling constants, negative specific rotation, and CD data ($[\theta]_{235}$ −21,400, $[\theta]_{280}$ −28,300) with those of rhusopolyphenol A ($[\theta]_{236}$ −15,200, $[\theta]_{274}$ −31,300) (Kim et al., 2013). Consequently, the structure of compound **2** was established as shown in Fig. 1, and named rhusopolyphenol H.

Compound **3** was obtained as a colorless gum. The HR-ESIMS data (*m/z* 359.1103 $[M+Na]^+$, calcd for $C_{17}H_{20}O_7Na$, 359.1107) of **3** indicated that this molecule possessed the molecular formula $C_{17}H_{20}O_7$ with 8 degrees of unsaturation. The ^1H and ^{13}C NMR spectra (Table 1) were remarkably similar to those of rhusopolyphenol A (Kim et al., 2013). The major difference was the presence of an ethoxy group at δ 3.75 (1H, q, J=7.5 Hz), 3.71 (1H, q, J=7.5 Hz) and δ 63.9; δ 1.24 (3H, t, J=7.5 Hz) and δ 14.7 with the aid of the HMQC experiment. The location of the ethoxy group was deduced by the HMBC correlation from the ethoxy protons (δ 3.75 and 3.71) to C-9 (δ 75.6). Full assignments of the ^1H and ^{13}C NMR spectra (Table 1) of **3** were carried out by the analysis of the COSY, HMQC, and HMBC data. The relative configuration of **3** was established as 7,8-*cis*- and 8,9-*cis*-orientation according to the smaller coupling constants ($J_{7,8}$=1.0 Hz and $J_{8,9}$=2.5 Hz) (Wiesler and Nakanishi, 1990), which was an unprecedented isomer in these types of compounds isolated from our previous research (Kim et al., 2013). Thus, the absolute configuration of **3** was determined by chemical methods and a CD data analysis. Compound **3** was converted to flavanol (**3a**) using a Mitsunobu cyclization (Scheme 1) (Krohn et al., 2009; Jew et al., 2000). Compound **3a** was identified as (+)-4-*O*-ethyl-mollisacacidin by its ^1H NMR, positive specific rotation, and MS data. The standard S_N2-type Mitsunobu reaction conditions were employed to obtain the enantioselective flavonol (Krohn et al., 2009), which was confirmed to be the expected 2,3-*trans*-3,4-*trans*-configuration in the ^1H NMR spectrum of **3a**. The CD spectrum of **3a** ($[\theta]_{238}$ −53,500, $[\theta]_{290}$ −45,100) established its absolute configuration to be 2*R*,3*S*,4*R*. (Ferreira et al., 2004). Thus, the absolute configuration of **3** was assigned 7*S*,8*R*,9*R* based on the absolute configuration of **3a** because a change in the configuration at C-2 and C-3 of **3a** occurs during the S_N2-type Mitsunobu reaction (Jew et al., 2000; Krohn et al., 2009; Kim et al., 2013). On the basis of these considerations, compound **3** was elucidated as shown in Fig. 1, named rhusopolyphenol I.

It was likely that compounds **1–3** were artifacts, not genuine natural products because the fermentation or hot water extraction may change some constitutions and structures of naturally occurring compounds. In order to verify if compounds **1–3** are authentic natural products, another supply of *Toxicodendron vernicifluum* bark was obtained and extracted with 50% EtOH and 80% MeOH in H_2O at room temperature. Both resulting extracts were tested using LC–MS analyses, alone and co-injected with the isolated compounds **1–3**. The peaks of the compounds were detectable in the LC–MS analyses of both crude extracts. These results proved that compounds **1–3** are genuine natural products.

Compound **4** was elucidated as 2-benzyl-2,3′,4′,6-tetrahydroxybenzo[*b*]furan-3(2*H*)-one by the interpretation of 2D NMR data including the COSY, HMQC, and HMBC spectra, which was previously reported from the heartwood of *Rhus succedanea* (Kondo and Imamura, 1985). But, the reported NMR data has not been accurate (Kondo and Imamura, 1985), so in this study, we report the corrected NMR assignments (Table 2) of **4**. Compound **4** existed as an enantiometirc pair ($[\alpha]_D^{25}$= 0) due to the reversible nature of hemiacetal at C-2 (Li et al., 1997). Compound **5** was identified as sulfuretin (Lee et al., 2002) by comparing their spectroscopic data with values reported previously. Compound **6** was identified as (+)-(2*S*,3*R*)-fustin (Park et al., 2000) by analysis of 2D NMR experiments, whose NMR data (Table 2) were reported in this study. The other known compounds were identified as (+)-epitaxifolin (**7**) (Kiehlmann and Li, 1995), butein (**8**), (Lee et al., 2002), and fisetin (**9**) (Harborne, 1994) by comparing their spectroscopic data with the values reported in the references.

3.2. Antiproliferative activity

Compounds **1–9** were evaluated for their antiproliferative activities against the A549, SK-OV-3, SK-MEL-2, and HCT-15 cell lines using the SRB bioassay (Skehan et al., 1990). Compounds **4–9** showed antiproliferative activity against the tested cells, with IC_{50} values of 4.78–28.89 μM (Table 3), but new compounds **1–3** were inactive (IC_{50} > 30.0 μM). These results were in agreement with the result that the presence of a ketone group at C-9 in molecules of **1–3** is essential for manifesting the cytotoxic activity (Kim et al., 2013). In general, compounds **5**, **8**, and **9** significantly inhibited cell proliferation in the SK-OV-3, SK-MEL-2, and HCT-15 cell lines with IC_{50} values of 7.43–9.51, 4.78–7.37, and 8.18–9.08 μM, respectively. Among them, recently, butein (**8**) was reported to exert potent anticancer activity by inhibiting angiogenesis of human endothelial progenitor cells via the translation dependent signaling pathway (Chung et al., 2013).

3.3. Anti-inflammatory activity

Studies using in vitro and in vivo models have demonstrated the anti-inflammatory effects of *Toxicodendron vernicifluum* (Choi et al., 2003; Jung et al., 2011), which was also confirmed by our preliminary work that the EtOH extract of *Toxicodendron vernicifluum* bark showed a significant inhibitory effect on NO production in the LPS-stimulated BV-2 microglial cell line. Microglial cells have been proposed to play a role in homeostasis regulation and defense against injury (Perry and Gordon, 1988). Under pathological conditions, microglia cells are over-activated and then produce a variety of proinflammatory mediators including NO (McGeer et al., 1993). Therefore, compounds **1–9** were evaluated

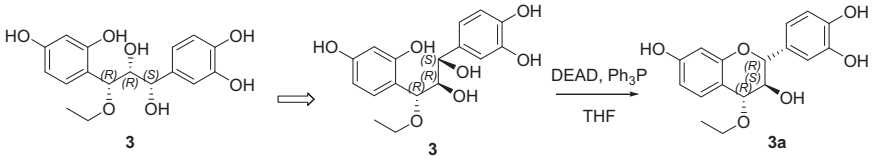

Scheme 1. Reagents and conditions: DEAD, Ph_3P, THF, 3 h.

Table 3
Antiproliferative activity of compounds **4–9** against four cultured human cancer cell lines in the SRB bioassay.

Compound	IC_{50} (μM)[a]			
	A549	SK-OV-3	SK-MEL-2	HCT-15
4	26.84 ± 1.02[b]	21.64 ± 0.41	11.39 ± 0.85	23.90 ± 0.63
5	12.71 ± 0.89	9.51 ± 0.72	7.43 ± 0.18	7.80 ± 1.46
6	26.57 ± 0.32	19.61 ± 1.27	17.14 ± 0.97	10.26 ± 0.26
7	22.67 ± 0.55	12.38 ± 1.31	20.13 ± 0.59	28.89 ± 1.10
8	10.22 ± 1.30	5.03 ± 1.08	7.37 ± 0.25	4.78 ± 1.13
9	17.16 ± 0.69	8.18 ± 0.15	8.92 ± 1.48	9.08 ± 0.72
Doxorubicin[c]	0.016 ± 0.005	0.027 ± 0.003	0.036 ± 0.001	1.073 ± 0.067

[a] 50% inhibitory concentration; the concentration of compound that caused a 50% inhibition in cell growth.
[b] Data are expressed as mean ± SEM of three independent experiments.
[c] Doxorubicin as a positive control.

Table 4
Inhibitory effects of compounds **1–9** on NO production in LPS-activated BV-2 cells.

Compound	IC_{50} (μM)[a]	Compound	IC_{50} (μM)[a]
1	37.82 ± 0.77[b]	**6**	100.22 ± 3.63
2	89.08 ± 4.79	**7**	80.43 ± 2.45
3	> 200	**8**	11.81 ± 0.80
4	66.98 ± 1.17	**9**	> 200
5	23.37 ± 2.39	**NMMA**[c]	12.77 ± 1.62

[a] IC_{50} value of each compound was defined as the concentration (μM) that caused 50% inhibition of NO production in LPS-activated BV-2 cells.
[b] Data are expressed as mean ± SEM of three independent experiments.
[c] NMMA was the positive control.

for anti-inflammatory activities by measuring NO levels in LPS-activated BV-2 cells. As shown in Table 4, compounds **1**, **4**, **5** and **8** inhibited NO production. Among them, compounds **5** and **8** significantly inhibited NO levels with IC_{50} values of 23.37 and 11.81 μM, respectively. Many studies have reported the anti-inflammatory activities of sulfuretin (**5**) and butein (**8**) (Song et al., 2010; Lee at al., 2012; Wang et al., 2014). Moreover, these compounds suppressed LPS-induced inflammatory responses in the murine macrophage RAW264.7 cells (Lee et al., 2004; Shin et al., 2010). According to these investigations, sulfuretin and butein dose-dependently reduced the production of NO and tumor necrosis factor-α, and the expression of inducible nitric oxide synthase (iNOS) and cyclooxygenase-2 via downregulation of nuclear factor-κB (NF-κB). Therefore, it is possible that the inhibitory effects of compounds **5** and **8** on NO production in LPS-activated BV-2 may be associated with reducing iNOS expression via suppressing NF-κB activation.

4. Conclusions

This study determined the structures of three new polyphenols, rhusopolyphenols G-I (**1–3**) and six known flavonoids present in the bark of *Toxicodendron vernicifluum* using bioactivity-guided isolation, spectroscopic data analysis, and chemical methods. Antiproliferative and anti-inflammatory assays of the isolated compounds revealed that compounds **5**, **8**, and **9** can be considered highly cytotoxic agents (IC_{50} values < 10 μM) in SK-OV-3, SK-MEL-2, and HCT-15 cell lines, and compounds **5** and **8** also exhibited anti-inflammatory effects by inhibiting NO production (IC_{50} values < 30 μM) in LPS-stimulated BV-2 cells. Taking into account that compounds **5** and **8** showed higher cytotoxic and anti-inflammatory activities, it could be concluded that some of the isolated compounds contribute to beneficial health effects and ethnopharmacological usage of *Toxicodendron vernicifluum* as anti-cancer and/or anti-inflammatory agents.

Acknowledgments

This work was supported by the Basic Science Research Program through the National Research Foundation of Korea (NRF) funded by the Ministry of Education, Science and Technology (2012R1A5A2A28671860). We thank Drs. E. J. Bang, S. G. Kim, and J. J. Seo at the Korea Basic Science Institute for their aid in the NMR and MS spectra measurements.

References

Choi, J., Yoon, B.J., Han, Y.N., Lee, K.T., Ha, J., Jung, H.J., Park, H.J., 2003. Antirheumatoid arthritis effect of *Rhus verniciflua* and of the active component, sulfuretin. Planta Medica 69, 899–904.
Chung, C.H., Chang, C.H., Chen, S.S., Wang, H.H., Yen, J.Y., Hsiao, C.J., Wu, N.L., Chen, Y.L., Huang, T.F., Wang, P.C., Yeh, H.I., Wang, S.W., 2013. Butein inhibits angiogenesis of human endothelial progenitor cells via the translation dependent signaling pathway. Evidence-Based Complementary and Alternative Medicine 2013, 943187.
Ferreira, D., Marais, J.P.J., Slade, D., Walker, L.A., 2004. Circular dichroic properties of flavan-3,4-diols. Journal of Natural Products 67, 174–178.
Harborne, J.B., 1994. Dictionary of Natural Products. vol. 9. Chapman & Hall, New York p. 5468.
Huh, J., 1999. Dong Ui Bo Gam. The Precious Mirror of Oriental Medicine. Namsandang; Seoul.
Jang, H.S., Kook, S.H., Son, Y.O., Kim, J.G., Jeon, Y.M., Jang, Y.S., Choi, K.C., Kim, J., Han, S.K., Lee, K.Y., Park, B.K., Cho, N.P., Lee, J.C., 2005. Flavonoids purified from *Rhus verniciflua* Stokes actively inhibit cell growth and induce apoptosis in human osteosarcoma cells. Biochimica et Biophysica Acta 1726, 309–316.
Jew, S., Kim, H., Bae, S., Kim, J., Park, H., 2000. Enantioselective synthetic method for 3-hydroxyflavanones: an approach to (2R,3R)-3′,4′-O-dimethyltaxifolin. Tetrahedron Letters 41, 7925–7928.
Jung, C.H., Kim, J.H., Kim, J.H., Chung, J.H., Choi, H.S., Seo, J.B., Shin, Y.C., Kim, S.H., Ko, S.G., 2011. Anti-inflammatory effect of *Rhus verniviflua* Stokes by suppression of iNOS-mediated Akt and ERK pathways: in-vitro and in-vivo studies. The Journal of Pharmacy and Pharmacology 63, 679–687.
Kiehlmann, E., Li, E.P.M., 1995. Isomerization of dihydroquercetin. Journal of Natural Products 58, 450–455.
Kim, H., 2000. Herbalogy. Young Lim Sa, Seoul.
Kim, J.H., Go, H.Y., Jin, D.H., Kim, H.P., Hong, M.H., Chung, W.Y., Park, J.H., Jang, J.B., Jung, H., Shin, Y.C., Kim, S.H., Ko, S.G., 2008. Inhibition of the PI3K-Akt/PKB survival pathway enhanced an ethanol extract of *Rhus verniciflua* Stokes-induced apoptosis via a mitochondrial pathway in AGS gastric cancer cell lines. Cancer Letters 265, 197–205.
Kim, J.H., Jung, C.H., Jang, B.H., Go, H.Y., Park, J.H., Choi, Y.K., Hong, S.I., Shin, Y.C., Ko, S.G., 2009. Selective cytotoxic effects on human cancer cell lines of phenolic-rich ethyl-acetate fraction from *Rhus verniciflua* Stokes. The American Journal of Chinese Medicine 37, 609–620.
Kim, K.H., Moon, E., Choi, S.U., Kim, S.Y., Lee, K.R., 2013. Polyphenols from the bark of *Rhus verniciflua* and their biological evaluation on antitumor and anti-inflammatory activities. Phytochemistry 92, 113–121.
Kim, T.Y., Yeo, S.H., Choi, H.S., Kim, J.S., 2011. Patent, Repub. Korean Kongkae Taeho Kongbo, KR 2011088692A 20110804.
Kondo, R., Imamura, H., 1985. The chemistry of the color of wood. I. The phenolic components of hazenoki (*Rhus succedanea* L.) and their dyeing properties. Mokuzai Gakkaishi 31, 927–934.
Krohn, K., Ahmeda, I., John, M., 2009. Enantioselective synthesis of flavan-3-ols using a Mitsunobu cyclization. Synthesis 5, 779–786.
Lee, S.K., Jung, H.S., Eo, W.K., Lee, S.Y., Kim, S.H., Shim, B.S., 2010. *Rhus verniciflua* Stokes extract as a potential option for treatment of metastatic renal cell carcinoma: report of two cases. Annals of Oncology 21, 1383–1385.
Lee, J.H., Lee, H.J., Choi, W.C., Yoon, S.W., Ko, S.G., Ahn, K.S., Choi, S.H., Lieske, J.C., Kim, S.H., 2009. *Rhus verniciflua* Stokes prevents cisplatin-induced cytotoxicity and reactive oxygen species production in MDCK-I renal cells and intact mice. Phytomedicine 16, 188–197.
Lee, J.C., Lim, K.T., Jang, Y.S., 2002. Identification of *Rhus verniciflua* Stokes compounds that exhibit free radical scavenging and anti-apoptotic properties. Biochimica et Biophysica Acta 1570, 181–191.
Lee, S.H., Seo, G.S., Sohn, D.H., 2004. Inhibition of lipopolysaccharide-induced expression of inducible nitric oxide synthase by butein in RAW 264.7 cells. Biochemical and Biophysical Research Communications 323, 125–132.
Lee, Y.R., Hwang, J.K., Koh, H.W., Jang, K.Y., Lee, J.H., Park, J.W., Park, B.H., 2012. Sulfuretin, a major flavonoid isolated from *Rhus verniciflua*, ameliorates experimental arthritis in mice. Life Sciences 90, 799–807.
Li, X., Cai, L., Wu, C.D., 1997. Antimicrobial compounds from *Ceanothus americanus* against oral pathogens. Phytochemistry 46, 97–102.

McGeer, P.L., Kawamata, T., Walker, D.G., Akiyama, H., Tooyama, I., McGeer, E.G., 1993. Microglia in degenerative neurological disease. Glia 7, 84–92.
Park, H.J., Kwon, S.H., Kim, G.T., Lee, K.T., Choi, J.H., Choi, J., Park, K.Y., 2000. Physicochemical and biological characteristics of flavonoids isolated from the heartwoods of *Rhus verniciflua*. Saengyak Hakhoechi 31, 345–350.
Perry, V.H., Gordon, S., 1988. Macrophages and microglia in the nervous system. Trends in Neurosciences 6, 273–277.
Reif, D.W., McCreedy, S.A., 1995. N-nitro-L-arginine and N-monomethyl-L-arginine exhibit a different pattern of inactivation toward the three nitric oxide synthases. Archives of Biochemistry and Biophysics 1, 170–176.
Samoszuk, M., Tan, J., Chorn, G., 2005. The chalcone butein from *Rhus verniciflua* Stokes inhibits clonogenic growth of human breast cancer cells co-cultured with fibroblasts. BMC Complementary and Alternative Medicine 5, 5.
Skehan, P., Storeng, R., Scudiero, D., Monks, A., MaMahon, J., Vistica, D., Warren, J.T., Bokesch, H., Kenney, S., Boyd, M.R., 1990. New colorimetric cytotoxicity assay for anticancer-drug screening. Journal of the National Cancer Institute 82, 1107–1112.
Son, Y.O., Lee, K.Y., Lee, J.C., Jang, H.S., Kim, J.G., Jeon, Y.M., Jang, Y.S., 2005. Selective antiproliferative and apoptotic effects of flavonoids purified from *Rhus verniciflua* Stokes on normal versus transformed hepatic cell lines. Toxicology Letters 155, 115–125.
Shin, J.S., Park, Y.M., Choi, J.H., Park, H.J., Shin, M.C., Lee, Y.S., Lee, K.T., 2010. Sulfuretin isolated from heartwood of *Rhus verniciflua* inhibits LPS-induced inducible nitric oxide synthase, cyclooxygenase-2, and pro-inflammatory cytokines expression via the down-regulation of NF-kappaB in RAW 264.7 murine macrophage cells. International Immunopharmacology 10, 943–950.
Song, M.Y., Jeong, G.S., Lee, H.S., Kwon, K.S., Lee, S.M., Park, J.W., Kim, Y.C., Park, B.H., 2010. Sulfuretin attenuates allergic airway inflammation in mice. Biochemical and Biophysical Research Communications 400, 83–88.
Wang, Z., Lee, Y., Eun, J.S., Bae, E.J., 2014. Inhibition of adipocyte inflammation and macrophage chemotaxis by butein. European Journal of Pharmacology 738C, 40–48.
Wiesler, W.T., Nakanishi, K., 1990. Relative and absolute configurational assignments of acyclic polyols by circular dichroism. 2. Determination of nondegenerate exciton coupling interactions by assignment of prochiral aryloxymethylene protons for proton NMR conformational analysis. Journal of the American Chemical Society 112, 5574–5583.